

## An X-ray study of the incommensurate structure in digenite ( $\text{Cu}_{1.8}\text{S}$ )

This article has been downloaded from IOPscience. Please scroll down to see the full text article.

1991 J. Phys.: Condens. Matter 3 6559

(<http://iopscience.iop.org/0953-8984/3/34/001>)

View [the table of contents for this issue](#), or go to the [journal homepage](#) for more

Download details:

IP Address: 171.66.16.147

The article was downloaded on 11/05/2010 at 12:29

Please note that [terms and conditions apply](#).

## An x-ray study of the incommensurate structure in digenite ( $\text{Cu}_{1.8}\text{S}$ )

S Kashida and K Yamamoto

Department of Physics, Niigata University, Ikarashi, Niigata, 950-21, Japan

Received 19 December 1990, in final form 17 April 1991

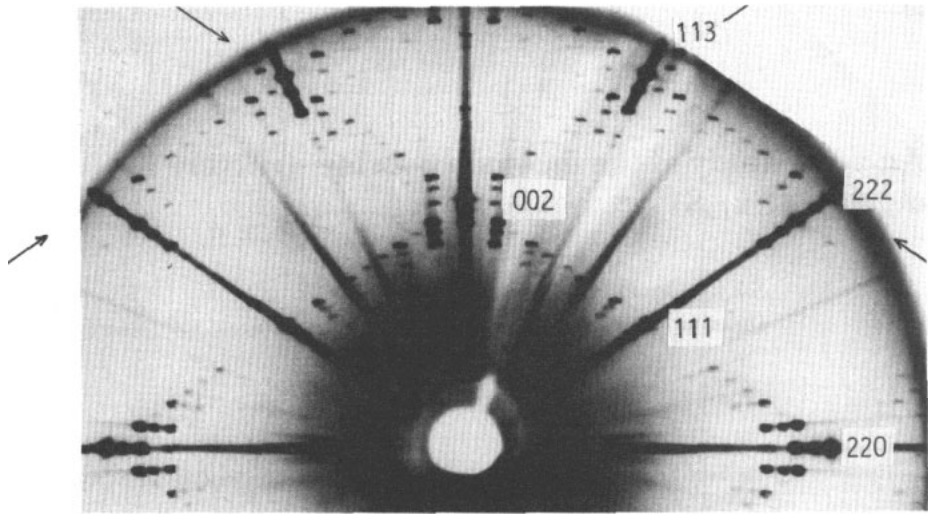
**Abstract.** The structure of a non-stoichiometric copper compound  $\text{Cu}_{1.8}\text{S}$  (digenite) has been studied by x-ray diffraction. Although digenite has a cubic anti-fluorite structure, satellite reflections were seen along the  $\langle 111 \rangle_c$  axis. Single-crystal x-ray diffraction data, including first- and second-order satellites, were collected using a four-circle diffractometer. A rhombohedral twinning model was used to determine the modulation densities of the copper ions. The final  $R$ -factor is about 10% including the main and satellite reflections. The present analysis shows that the crystal is composed of domain-like structures: in each domain, the dimensions of the regular lattice, formed from copper ions, are slightly larger than those of the basic sulphur lattice. The origin of this domain-like structure, based on the Frenkel–Kontorova model, is attributed to the non-stoichiometry and apparently smaller cation–anion interaction.

### 1. Introduction

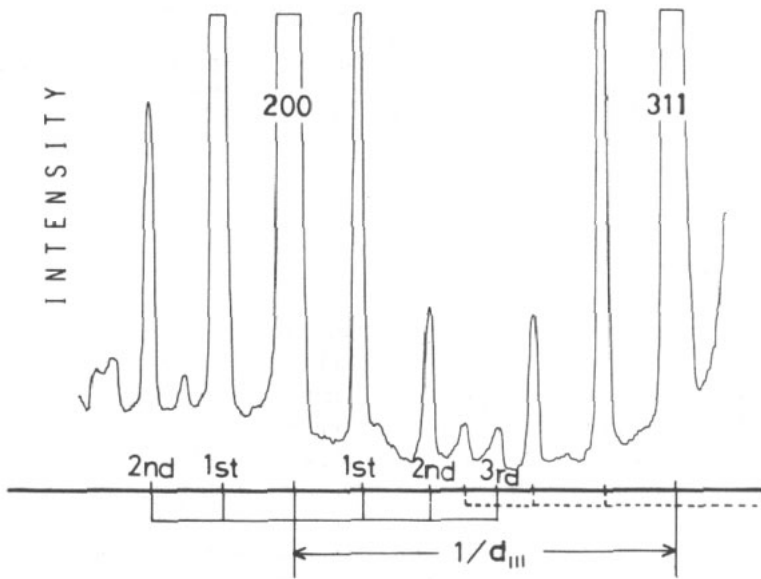
Compounds of the copper–sulphur system are useful minerals, and their mineralogical and technological properties have been studied extensively. The compounds exhibit fast-ion conduction at high temperatures. Digenite,  $\text{Cu}_{2-x}\text{S}$  (where  $x$  ranges from about 0.18 to 0.25) belongs to this family. Its high temperature structure is characterized by ‘immobile’ sulphur cages which have cubic close-packed layers in which ‘mobile’ copper ions are randomly distributed over the tetrahedral and trigonal interstices of the anions [1].

Upon cooling, digenite undergoes a phase transition around 80 °C, below which the copper ions have an ordered configuration. At room temperature, digenite shows satellite reflections indicating modulation along the body diagonal of the cube (figure 1) [2, 3]. This modulation is attributed to an ordering of vacant copper sites, since the wavelength depends upon composition and varies from 5 to 6 [4]. The structure of digenite has been investigated [5, 6], in a number of studies to the authors’ knowledge, however, no detailed analysis of the structure has been reported.

The aim of the present paper is to report precise data for the digenite structure. We have prepared a crystal that has an incommensurate  $5.5a$  structure. In order to collect the intensity data of very weak satellite reflections, a four-circle x-ray diffractometer was used. In the refinement, the least squares program ‘REMOS’ [7] was used, and Fourier synthesis was employed effectively as well.



(a)



(b)

**Figure 1.** (a) Precession photograph of the  $(110)_c$  plane of digenite (type 5.5a) Cu  $K_\alpha$  radiation, without filter. Satellite reflections appear only along the lines marked by arrows (reflections in other places are due to  $K_\beta$  radiation). (b) A photometer trace of the photograph in (a); note that the lower angle satellite is stronger than the higher angle one. The intensities of the main and first satellite are over-scaled.

**Table 1.** Crystal data of  $Cu_{1.8}S$  (5.5a type) at 300 K. The standard errors are in parentheses.

Lattice constants	Absorption coefficients	Sample dimensions
5.555(3) Å	$\mu = 244 \text{ cm}^{-1}$	$0.38 \times 0.27 \times 0.36 \text{ mm}^3$

## 2. Experimental procedure

Digenite crystals ( $Cu_{2-x}S$  with  $x \sim 0.2$ ) were prepared by direct reaction of the elements: the weighted components, sulphur (99.999%) and copper (99.99%) were sealed in an evacuated silica tube. The mixture was gradually heated to 700 °C, kept at that temperature for about one week and then cooled to room temperature over five hours. The crystals obtained were shiny black distorted cubo-octahedrons terminated by  $\langle 111 \rangle_c$  and  $\langle 100 \rangle_c$  planes.

Preliminary checks of the samples were made by taking precession photographs. Most crystals showed fundamental reflections indicating that the fundamental structure was of the FCC type. However, in the  $\langle 110 \rangle_c$  photographs, crystals with compositions around  $x = 0.2$  showed several kinds of satellite pattern; from the distances between the satellites, the unit-cell dimensions were estimated to be a factor of  $\sim 4-6$  greater along the  $\langle 111 \rangle_c$  axis. The crystal with the four-fold superlattice structure is classified as anilite [8] and the crystals with  $5 \sim 6a$  periods are classified as digenite. Other crystals had a different pattern that belongs to the hexagonal djurleite structure [9]. In a previous study of this system, Morimoto and Koto [4] reported that digenite is metastable at room temperature and decomposes to mixtures of anilite and djurleite. Single crystal samples of digenite were selected for the intensity measurement. A typical example of the photographs is shown in figure 1.

The x-ray diffraction intensities were collected using an automatic single-crystal diffractometer assembled in our laboratory. The main part of the diffractometer [10] consisted of a Huber four-circle goniometer. A Mo target was used with a flat graphite monochromator.

The unit cell parameters were derived by a least-squares method from 18 reflections within the range  $23^\circ < 2\theta < 38^\circ$ . The obtained unit-cell parameters are given in table 1. The integrated intensity was collected by the omega scan method. Due to imperfections, such as vacancies and dislocations in the crystal, the observed Bragg reflections were distorted and the scan range was wider than the usual value of  $3^\circ$ . The scanning rate was  $0.5^\circ \text{ min}^{-1}$  and the background count was measured for 20 s at each limit of the scan range. The intensities of the main, the first-order and second-order satellite reflections, which had indices  $h_c, k_c, l_c \geq 0$ , were collected up to the  $2\theta$  value of  $60^\circ$ .

In total, 1393 reflections were scanned and the intensities of equivalent reflections were averaged. The number of independent reflections, with intensities larger than the standard deviation, was 20 for the main, and 50 and 10 for the first- and second-order satellite reflections, respectively. As the number of second-order satellite reflections was not sufficient, we have also used an additional 40 reflections whose intensities are larger than  $\frac{1}{2}$  of the standard deviation. Although these are large standard deviations, the intensities of equivalent reflections are in good agreement and therefore can be used. The agreement factor of equivalent reflections, which is defined by  $\Sigma(|F_0| - |\bar{F}_0|)/\Sigma|F_0|$ , is around 0.10. The data were corrected for Lorentz and polarization effects. Absorption

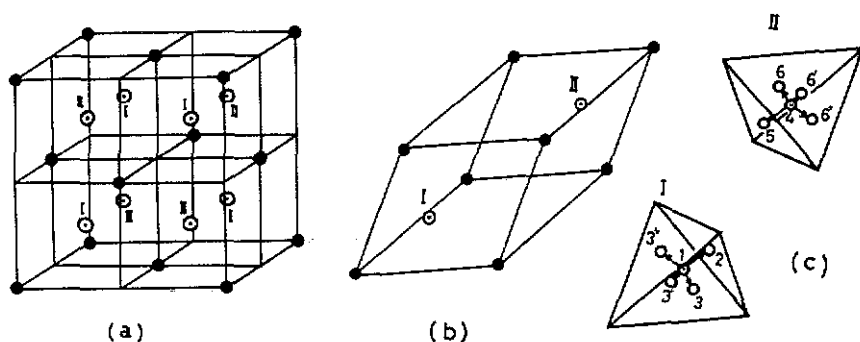


**Figure 2.** (a) Atomic arrangement in the fluorite structure. (b) Rhombohedral subcell taken in the analysis. (c) Copper distribution in sulphur tetrahedra: (1 and 4) tetrahedral sites, (2, 3, 5 and 6) trigonal sites. For clarity only the tetrahedral sites are drawn in (a) and (b). In space group  $R\bar{3}m$ , the trigonal sites 3, 3' and 3'', and 6, 6' and 6'' are equivalent, respectively. Note two different types of copper arrangement around the sites I and II.

correction was made by assuming a polyhedral shape of the specimen, the absorption coefficient and the approximate dimensions of the sample are given in table 1.

### 3. Analysis of the structure

As shown by the x-ray photograph in figure 1, the diffraction pattern of digenite has several remarkable features:

(i) The satellite reflections show a special extinction rule: the satellites appear along the  $(111)^*$  reciprocal lattice direction and equivalent directions connecting the main reflections, but do not appear at their crossing points. Donnay *et al* [2] attributed this special extinction to the pseudo-cubic twinning of rhombohedral crystals.

(ii) The position of the satellite reflections is not located at a simple fraction of the reciprocal cells; in the present sample it is about  $1/5.5$ . This period varies with chemical composition in the range from 5.0 to 6.0 [4]; it is also reported to vary slightly with temperature [5]. The composition dependence strongly suggests that modulation is due to ordering of copper vacancies.

(iii) Asymmetry of intensities exists between pairs of satellites centred about the main reflections; the intensity of lower angle satellite is stronger than that of the higher angle one. As discussed by Guinier [11], the asymmetry suggests that modulation of atomic densities is accompanied by modulation of the positional parameters; larger atomic densities are accompanied by larger lattice constants. This is not compatible with a simple model of distribution of copper vacancies, because in this model there will be zero or negative correlation between atomic density and the lattice constants. Near the vacancy, atomic density is low and binding is weak, therefore lattice constants will be wider. The experimental results, however, suggest that copper-rich regions co-exist that have larger cell constants and vacancy-rich regions having smaller cell constants. This is reminiscent of 'spinodal decomposition' in solid solutions.

The 'average' structure was analysed using the intensities of the main reflections [12]. The copper ions were located at the tetrahedral and trigonal interstitial sites and these were numbered as shown in figure 2. The next problem would be arranging the copper

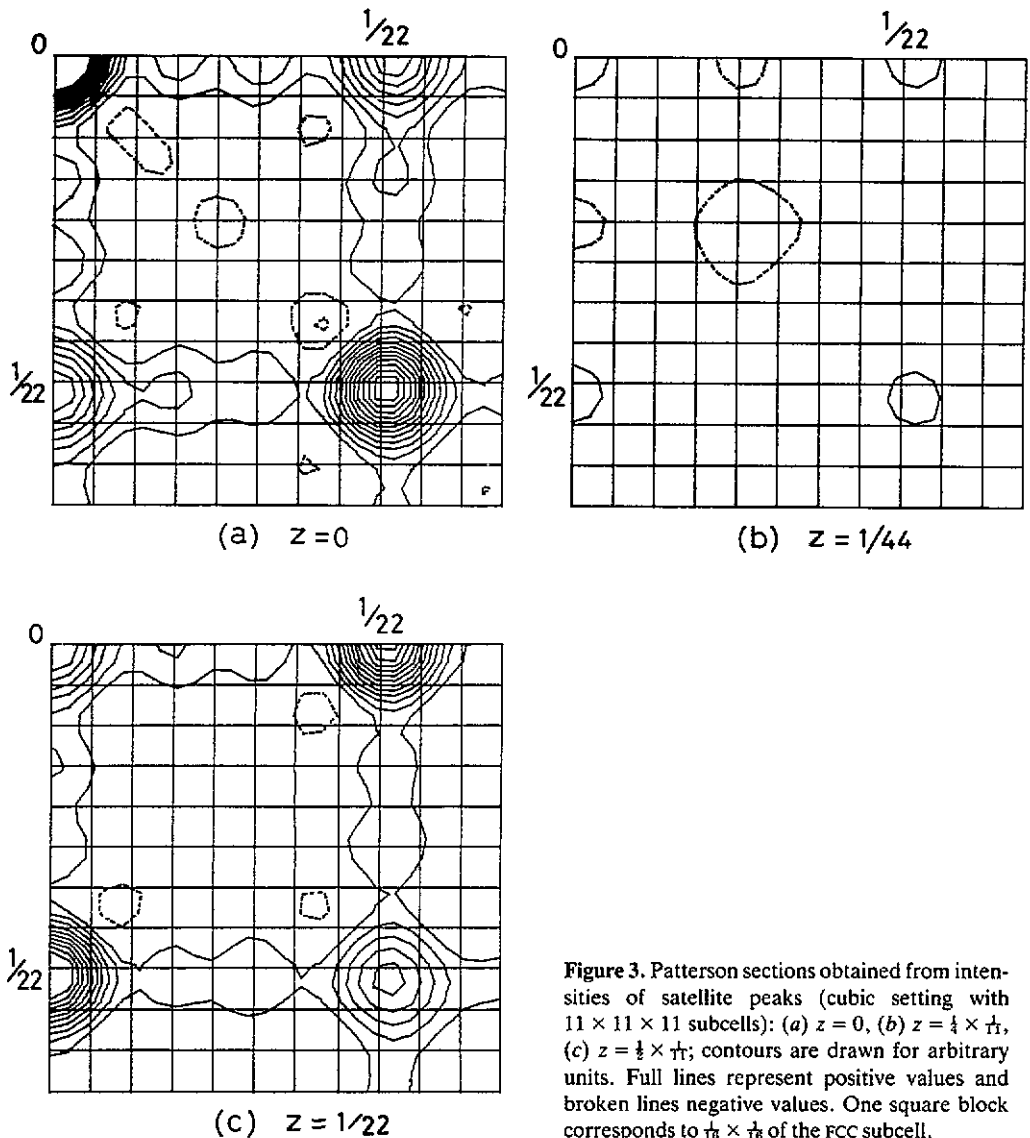


Figure 3. Patterson sections obtained from intensities of satellite peaks (cubic setting with  $11 \times 11 \times 11$  subcells): (a)  $z = 0$ , (b)  $z = \frac{1}{4} \times \frac{1}{11}$ , (c)  $z = \frac{1}{2} \times \frac{1}{11}$ ; contours are drawn for arbitrary units. Full lines represent positive values and broken lines negative values. One square block corresponds to  $\frac{1}{16} \times \frac{1}{16}$  of the FCC subcell.

atoms periodically on these sites. In order to obtain information about the arrangement, a partial Patterson function [13] was synthesized, where only the intensities of satellite reflections were used. This function is a self-convolution of the 'difference structure',  $\Delta\rho = \rho(\text{super-structure}) - \rho(\text{sub-structure})$ ; positive peaks correspond to occupied-occupied or vacant-vacant pairs, and negative peaks correspond to occupied-vacant pairs. The satellite reflections were indexed in terms of a cubic unit cell having dimensions  $11a \times 11a \times 11a$ .

Figure 3 shows three sections of the partial Patterson map at  $z = 0$ ,  $z = \frac{1}{4} \times \frac{1}{11}$  and  $z = \frac{1}{2} \times \frac{1}{11}$ . Only portions near the origin were drawn to check the local ordering. In table 2, the peaks listed are assigned to correlations between the sites of the first to third

**Table 2.** Peak values of the partial Patterson function. The values represent relative height, where the value at the origin is normalized to 1.

First		Second		Third	
$F_1^4$	0.354	$S_{1-3}^+$	0.569	$T_1^+$	0.249
$F_1^5$	-0.089	$S_1^3$	-0.055	$T_1^+$	-0.056
$F_2^3$	0.105	$S_1^3$	-0.111	$T_2^0$	0.086
$F_2^6$	0.105	$S_2^3$	-0.038	$T_3^0$	-0.034
$F_3^5$	-0.036	$S_2^3$	-0.046	$T_3^0$	0.057
$F_3^6$	0.075	$S_3^3$	-0.028		

neighbours (on the scale of the tetrahedral copper sites). The following points were noted about the local order:

(i) There is a simple cubic array of positive peaks, as seen in the sections at  $z = 0$  and  $z = \frac{1}{2}$ . These peaks are attributed to copper-copper pairs. Copper atoms form a simple cubic array in the fluorite structure. The contour map at  $z = \frac{1}{4}$  shows that the correlation between the copper and sulphur ions is rather weak.

(ii) The peak at the second-neighbour site is stronger than those at the first- and third-neighbour sites. However, some of the second neighbour peak height may be attributed to the correlation between the sulphur atoms; the second-neighbour copper correlation will be stronger than that of the first neighbour or the third neighbour. This is consistent with the argument that the crystal has a tendency to form zinc-blende type lattices [14], or to form octahedral clusters that are made of vacancies at the second-neighbour tetrahedral sites [15]. As discussed in the next section, however, this is a natural consequence of modulation being along the  $\langle 111 \rangle_c$  axis.

(iii) Positive sub-peaks are observed near the first- and third-neighbour peaks, and negative peaks are observed in the inside regions of the first- to third-neighbour peaks. The positive peaks suggest occupations of the trigonal sites, and the negative peaks suggest that ions in the trigonal sites are attracted by a tetrahedral vacancy at nearby positions.

The information obtained by the partial Patterson function is useful to deduce the local structure. It would, however, not be sufficient to determine the structure by the ordinary method: the number of available reflections is only 80 ~ 120, whereas there are too many atoms in the  $11a \times 11a \times 11a$  unit cell. Therefore, another approach was used to determine the modulation waves caused in the crystal. This gave a coarse-grained picture of the digenite structure.

In the refinement, the least squares program 'REMOS' [7] was used. For simplicity the rhombohedral twinning model originally presented for Donnay *et al* [2] was used. A rhombohedral primitive cell was taken as the base structure, of which the hexagonal axis was along the body diagonal of the FCC lattice (see figure 2). The space group  $R\bar{3}m$  was chosen instead of  $R3m$  as proposed by Donnay *et al* [2]; we explain why in the next section. Atoms were distributed at the following sites, given in table 3 (see also figure 2); this 'average' structure preserves cubic face-centred symmetry.

At first, only the modulation of ionic copper densities was taken into account, where harmonics were taken up to the second order. There was no extinction rule in this setting, therefore the parameters were not restricted. In the refinement, all reflections were

**Table 3.** Positional parameters of the average structure.  $\xi = 0.327 \approx \frac{1}{3}$ .

Atom	Site	Position	Average population
S	(1a)	(0, 0, 0)	1.000
Cu-1	(1a)	( $\frac{1}{3}, \frac{1}{3}, \frac{1}{3}$ )	0.520
Cu-4	(1a)	( $\frac{2}{3}, \frac{2}{3}, \frac{2}{3}$ )	0.520
Cu-2	(1a)	( $\xi, \xi, \xi$ )	0.095
Cu-5	(1a)	( $1 - \xi, 1 - \xi, 1 - \xi$ )	0.095
Cu-3	(3b)	( $\xi, \xi, 1 - 3\xi$ )	0.285
Cu-6	(3b)	( $1 - \xi, 1 - \xi, 3\xi$ )	0.285

**Table 4.** Modulation functions for the population and thermal parameters. The form of the thermal parameter is  $\exp[-(B/4)(2 \sin \theta/\lambda)^2]$ . Average values of the populations (constant terms) are normalized to 1. The standard errors are in parentheses.

Atom	Const. term	$\cos 2\pi x$	$\sin \pi x$	$\cos 4\pi x$	$\sin 4\pi x$
S	P 1.000				
	B 1.63(9)				
Cu-1	P 1.00(4)	0.44(6)	0.60(5)	-0.00(5)	0.10(8)
	B 6.71(28)	-3.40(41)	-1.60(44)	0.24(53)	1.89(45)
Cu-4	P 1.00(4)	0.21(4)	-0.01(4)	-0.30(4)	-0.19(5)
	B 4.63(12)	1.49(24)	-2.91(13)	0.53(21)	2.32(14)
Cu-2	P 1.00(13)	-1.06(22)	0.05(23)	-0.11(25)	-0.16(24)
	B 3.23(78)				
Cu-5	P 1.00(10)	-0.75(17)	-0.61(17)	0.51(21)	0.07(17)
	B 0.84(39)				
Cu-3	P 1.00(6)	-0.13(9)	-0.73(11)	-0.21(11)	0.13(11)
	B 1.38(27)				
Cu-6	P 1.00(8)	-0.10(13)	0.31(9)	0.07(10)	0.42(13)
	B 2.01(34)				
No. of reflections					
Total (120)	Main (20)	1st (50)	2nd (50)		
$R = 0.108$	$R^0 = 0.075$	$R^1 = 0.107$	$R^2 = 0.181$		

given unit weight and isotropic temperature factors were used for all atoms. The scattering factors used are those listed in [16].

The least squares calculation was performed using the atomic positions of the 'average' structure and zero values for the displacive modulation amplitudes of the copper atoms as initial parameters. In the course of refinement, the  $R$ -factor was reduced to about 15%. However, some of the atoms in the trigonal sites were found to yield negative temperature factors. This problem was settled by introducing modulations of the temperature factor for atoms in the tetrahedral sites reducing the  $R$ -factor further. The final  $R$ -factor and the relevant parameters are given in table 4, where  $R = \Sigma(|F_0| - |F_c|) / \Sigma|F_0|$ .



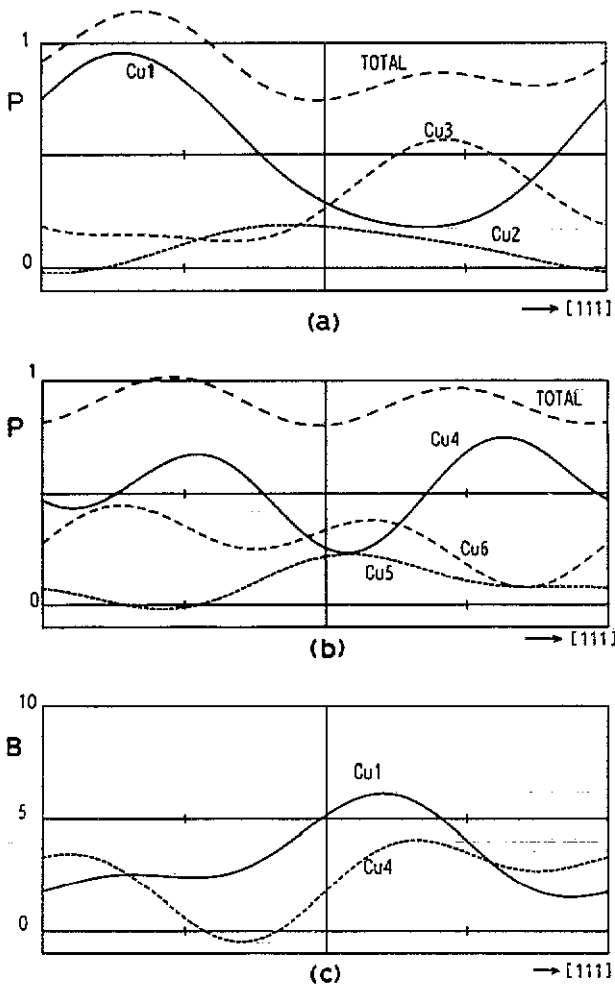


Figure 4. Modulation functions for the population and thermal parameters over 5.5 subcells; (a), (b) population; (c) thermal parameter. The population of the copper ions is normalized to 0.9, the definition of the thermal parameter  $B$  is the same as in table 4.

#### 4. Description of the structure and discussion

Figure 4 shows the calculated pattern of the modulation functions. Note the following points concerning the density modulation of copper ions:

(i) The populations of the two tetrahedral sites (Cu1 and Cu4) do not change in-phase, hence the non-centro-symmetric space group  $R\bar{3}m$  was selected. This also implies that the second-neighbour cation correlation is much stronger than the first or the third. As figure 2 shows, the second-neighbour correlation is taken between the sites of the same type belonging to different cells (I-I or II-II, such as Cu1-Cu1 or Cu4-Cu4, etc), whereas the first- or the third-neighbour correlation is taken between sites belonging to different types (I-II, such as Cu1-Cu4).

(ii) The populations of two trigonal sites, Cu3 and Cu5, are  $180^\circ$  out of phase so as to compensate for the decrease in the populations of tetrahedral sites, while the populations of other trigonal sites, Cu2 and Cu6, seem to change in quadrature.

(iii) The temperature factor is larger when the population is low; this means that the deduced temperature factor is affected largely by configurational disorder rather than the normal thermal vibrations.

In order to get a perspective and more realistic view of the structure, a Fourier map was synthesized (see figure 5). This map clearly shows that the density modulation of copper ions plays an essential part in the digenite structure, this point has already been mentioned by many researchers [2–6]. Note, now, that the crystal has a domain-like structure.

(i) In each domain, copper ions form a regular lattice whose dimensions are slightly larger than those of the base structure: its principal axis is also slightly inclined to that of the base structure.

(ii) The domains are separated by dislocation regions, where the population of copper ions is relatively low and the effective cell constant is also small (see figures 5(d) and 5(f)). Thus, the dislocation regions compensate for the relatively large population and large cell constant within the coherent domains.

The mechanism of the incommensuration in the present system should be very similar to that studied by Frenkel and Kontorova [17]. In  $\text{Cu}_{1.8}\text{S}$ , the number of copper ions is somewhat smaller than the number of sulphur ions. If the cation–anion interaction is ignored, the coulombic repulsion should cause the copper ions to be distributed uniformly in the crystal; an ideal incommensurate structure where copper ions and sulphur ions form ‘independent lattices’ in a crystal. The interaction between the copper and sulphur ions plays the role of commensurability energy that modifies each lattice. The resultant arrangement tends to alter the phases of copper ions so they coincide locally with those of the basic sulphur lattice.

Under such circumstances, copper ions are distributed over the tetrahedral and trigonal interstices of sulphur ions. Preferential occupation of these sites maintains the distance between copper ions at that of ‘independent lattices’. This also causes inclination of the axis within a domain (see figure 5). The domain-like structure explains the asymmetry of the satellite reflections; it suggests the coexistence of copper-rich regions having larger lattice constants, and copper-poor regions having smaller lattice constants, as mentioned in the previous section.

In the present model, only the modulation along the  $\langle 111 \rangle_c$  axis was taken into account. In a real crystal, however, modulation occurs along each of the four equivalent directions simultaneously. In order to compare the present results with those of other experiments, such as electron microscopic studies, the density of copper ions was calculated taking into account two modulation waves travelling along the  $\langle 111 \rangle_c$  and  $\langle \bar{1}\bar{1}1 \rangle_c$  axes. Figure 6 shows the calculated density of copper ions projected onto the  $(1\bar{1}0)_c$  layer. The pattern qualitatively reproduces observations by Pierce and Buseck [14] showing alternating regions of copper-rich and vacancy-rich sites. The special extinction rule suggests that there is no long-range correlation between the modulation waves travelling along different directions. However, the long-range correlation will develop with time: by storing the crystal for a certain time at room temperature, the extinction rule was found to break [3, 14, 15]. In fact, as figure 1 shows, we could discern very weak reflections at cross points of the first-order satellites. The real space group is, therefore, not four dimensional  $P_{11}^{R3m}$  but six dimensional  $Fm\bar{3}m(\alpha, \alpha, \alpha)$  [18].

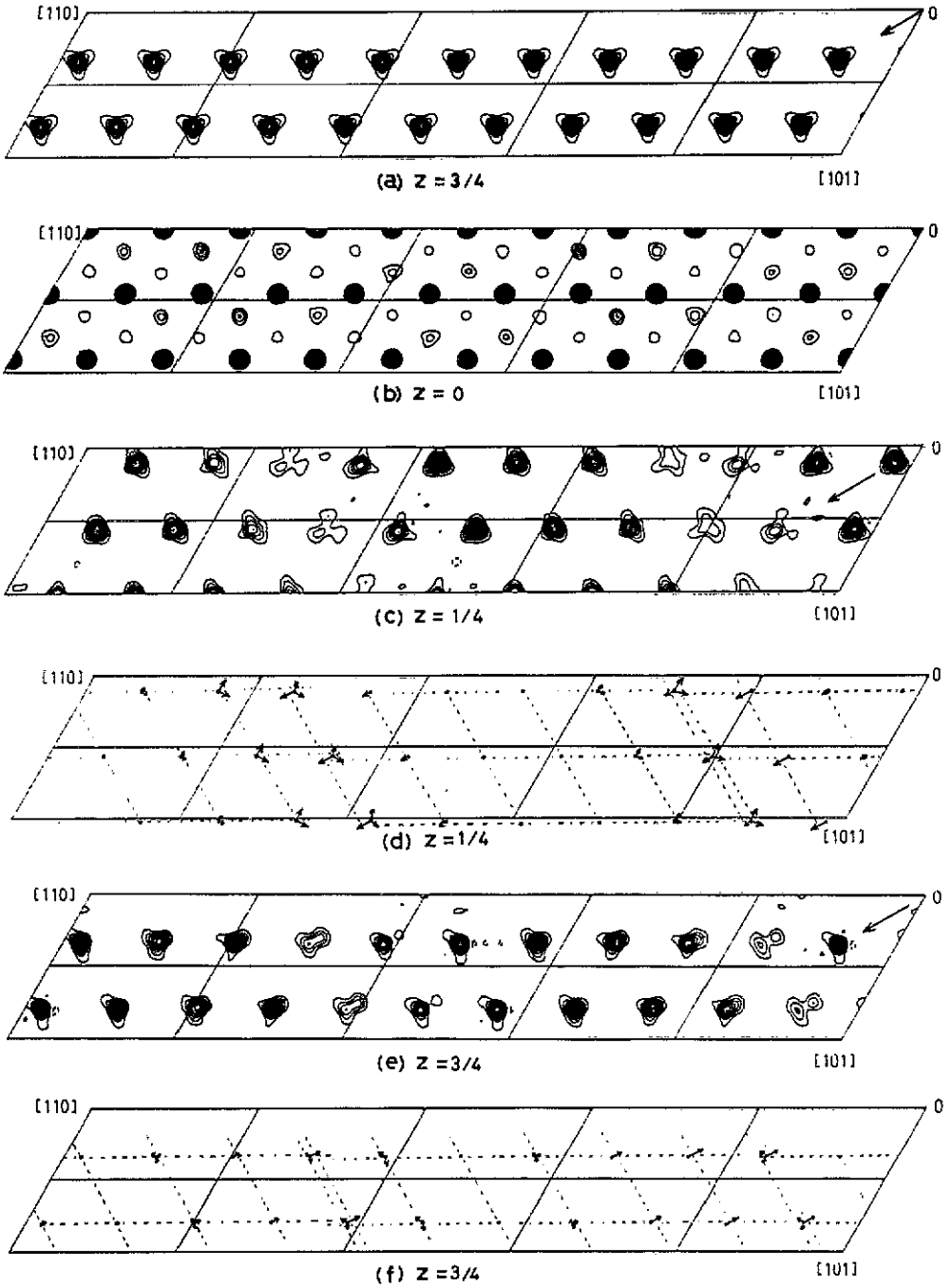


**Figure 5.** Fourier sections of  $(\bar{1}11)_c$  planes representing modulation over 11 subcells; (a) average structure; (b)–(e) modulated structure. Contours are drawn at intervals of  $5e/A^{-3}$ . The direction of modulation is taken along the  $\langle 111 \rangle_c$  axis, and its projected direction is marked by large arrows: (a)  $z = \frac{3}{4}$ , 'average' structure of copper ions; (b)  $z = 0$ , arrangement of sulphur ions in a  $(\bar{1}11)$  layer; (c), (e) modulated structure of copper ions in successive  $(\bar{1}11)_c$  layers. (d), (f) schematic representation of copper ion displacement in (c), (e).  $z$  is given in units of the rhombohedral subcell.

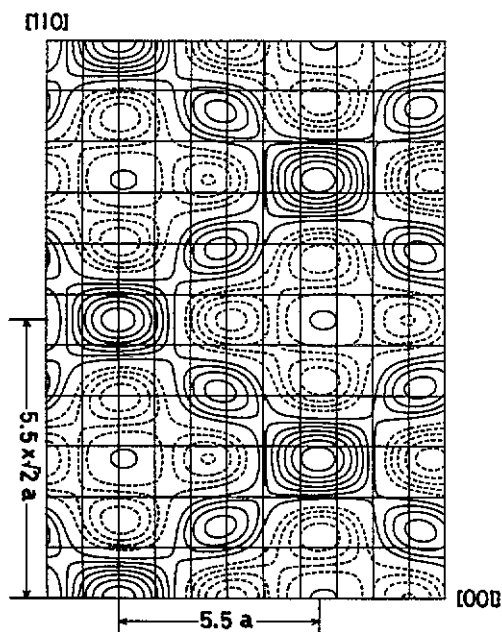


Figure 6. The calculated density of copper ions projected onto a  $(\bar{1}\bar{1}0)$  plane: two modulation waves are taken into account that travel along the  $\langle 111 \rangle$ , and  $\langle \bar{1}\bar{1}1 \rangle$ , axes. Full curves indicate copper-rich regions and broken curves vacancy-rich regions, contours are drawn for arbitrary units.

Using the twinning model of Donnay *et al* [2], the incommensurate structure of a digenite crystal has been analysed. We are quite confident about having identified most prominent features of the arrangement of copper ions, that is, a solution of the three-dimensional Frenkel-Kontorova model. The  $R$ -factor obtained is, however, still high when compared with the structural refinement standard. This may be due to several reasons:

- (i) The intensities of the satellite reflections are very weak and have large standard deviation (especially the second-order satellites).
- (ii) The interaction between the modulation waves travelling along different directions are neglected.

In order to construct a more precise model, the interaction between the modulation waves must be considered. Precise data for many higher order satellite reflections, not available here, would also be required.

### Acknowledgments

The authors are indebted to Dr A Yamamoto, National Institute for Research in Inorganic Materials, for supplying his software program 'REMOS'. They also thank Dr S Sato, Institute for Solid State Physics, University of Tokyo, for kind cooperation in the early stages of the experiment.

### References

- [1] Rahlfs P 1936 *Z. Phys. Chem. B* **31** 157

- [2] Donnay G, Donnay J D H and Kullerud G 1958 *Am. Mineral.* **43** 228
- [3] Morimoto N and Kullerud G 1963 *Am. Mineral.* **48** 110
- [4] Morimoto N and Koto K 1970 *Am. Mineral.* **55** 106
- [5] Gezalov M A 1982 *Sov. Phys.-Solid State* **23** 1863
- [6] Gray J N and Clarke R 1985 *Phys. Rev. B* **33** 2056
- [7] Yamamoto A 1982 *Acta Crystallogr. A* **38** 87
- [8] Koto K and Morimoto N 1970 *Acta Crystallogr. B* **26** 915
- [9] Evans Jr H T 1981 *Am. Mineral.* **66** 807
- [10] Kashida S and Yamamoto K 1990 *J. Solid State Chem.* **86** 180
- [11] Guinier A 1964 *Theorie et Technique de la Radiocristallographie* (Paris: Dunod)
- [12] Yamamoto K and Kashida S 1990 *J. Solid State Chem.* submitted
- [13] Koch F and Cohen J B 1969 *Acta Crystallogr. B* **25** 275
- [14] Pierce L and Buseck P 1978 *Am. Mineral.* **63** 1
- [15] Van Dyck D, Conde-Amiano C and Amelinckx S 1980 *Phys. Status Solidi* **58** 451
- [16] 1974 *International Tables for X-ray Crystallography* (Birmingham: Kinoch)
- [17] Frenkel Y I and Kontorova T 1938 *Zh. Eksp. Teor. Fiz.* **8** 1340
- [18] Janner A, Janssen T and de Wolff P M 1983 *Acta Crystallogr. A* **39** 671